

Multi-wavelength observations of Galactic hard X-ray sources discovered by *INTEGRAL* [★]

II. The environment of the companion star

F. Rahoui^{1,2}, S. Chaty², P-O. Lagage², and E. Pantin²

¹ European Southern Observatory, Alonso de Córdova 3107, Vitacura, Santiago de Chile
e-mail: frahoui@eso.org

² Laboratoire AIM, CEA/DSM - CNRS - Université Paris Diderot, IRFU/Service d'Astrophysique, Bât. 709, CEA-Saclay, F-91191 Gif-sur-Yvette Cédex, France

Received ; accepted

ABSTRACT

Context. The *INTEGRAL* mission has led to the discovery of a new type of supergiant X-ray binaries (SGXBs), whose physical properties differ from those of previously known SGXBs. Those sources are in the course of being unveiled by means of multi-wavelength X-rays, optical, near- and mid-infrared observations, and two classes are appearing. The first class consists of obscured persistent SGXBs and the second is populated by the so-called supergiant fast X-ray transients (SFXTs).

Aims. We report here mid-infrared (MIR) observations of the companion stars of twelve SGXBs from these two classes in order to assess the contribution of the star and the material enshrouding the system to the total emission.

Methods. We used data from observations we carried out at ESO/VLT with VISIR, as well as archival and published data, to perform broad-band spectral energy distributions of the companion stars and fitted them with a combination of two black bodies representing the star and a MIR excess due to the absorbing material enshrouding the star, if there was any.

Results. We detect a MIR excess in the emission of IGR J16318-4848, IGR J16358-4726, and perhaps IGR J16195-4945. The other sources do not exhibit any MIR excess even when the intrinsic absorption is very high. Indeed, the stellar winds of supergiant stars are not suitable for dust production, and we show that this behaviour is not changed by the presence of the compact object. Concerning IGR J16318-4848 and probably IGR J16358-4726, the MIR excess can be explained by their sgB[e] nature and the presence of an equatorial disk around the supergiant companion in which dust can be produced. Moreover, our results suggest that some of the supergiant stars in those systems could exhibit an absorption excess compared to isolated supergiant stars, this excess being possibly partly due to the photoionisation of their stellar wind in the vicinity of their atmosphere. (abridged)

Key words. Infrared: stars – X-rays: binaries, individuals: IGR J16195-4945, IGR J16207-5129, IGR J16318-4848, IGR J16320-4751, IGR J16358-4726, IGR J16418-4532, IGR J16465-4507, IGR J16479-4514, IGR J17252-3616, IGR J17391-3021, IGR J17544-2619, IGR J19140+0951 – binaries: general – supergiants – Stars: fundamental parameters

1. Introduction

High-mass X-ray binaries (HMXBs) are X-ray sources for which high-energy emission stems from accretion onto a compact object (black hole or neutron star) of material coming from a massive companion star. Until recently, the huge majority of known HMXBs were Be/X-ray binaries, i.e. a neutron star accreting from a disc around a Be star. Most of these sources are transient, even if a few are persistent weak X-ray emitters

($L_X \sim 10^{34}$ erg s⁻¹). The other known HMXBs were supergiant X-ray binaries (SGXBs), composed of a compact object orbiting around an early-type supergiant and fed by accretion from the strong radiative wind of the companion. These objects are persistent sources ($L_X \sim 10^{36}$ erg s⁻¹), and their relative low number compared to the population of Be/X-ray binaries was explained as the consequence of the short lifetime of supergiant stars.

The launch of the *INTERNATIONAL GAMMA-RAY ASTROPHYSICS LABORATORY (INTEGRAL)*, Winkler et al. 2003) in October 2002 completely changed the situation, as many more HMXBs whose companion stars are supergiants were

Send offprint requests to: F. Rahoui

[★] Based on observations carried out at the European Southern Observatory under programmes ID 075.D-0773 and 077.D-0721.

discovered during the monitoring of the Galactic centre and the Galactic plane using the onboard IBIS/ISGRI instruments (Ubertini et al. 2003; Lebrun et al. 2003). Most of these sources are reported in Bird et al. (2007) and Bodaghee et al. (2007), and their studies have revealed two main features that were not present on previously known SGXBs:

- first, many of them exhibit a considerable intrinsic absorption, with a column density up to $N_{\text{H}} \sim 2 \times 10^{24} \text{ cm}^{-2}$ in the case of IGR J16318-4848 (Matt & Guainazzi 2003), which explains why previous high-energy missions had not detected them.
- second, some of these new sources reveal a transitory nature. They are undetectable most of the time and occasionally present a fast X-Ray transient activity lasting a few hours. Moreover, they exhibit a quiescent luminosity of $L_{\text{X}} \sim 10^{33} \text{ erg s}^{-1}$, well below the persistent state of other SGXBs.

It then appears that the supergiant HMXBs discovered by *INTEGRAL* can be classified in two classes: one class of considerably obscured persistent sources that we will simply call obscured SGXBs in this paper and another of supergiant fast X-ray transients (SFXTs, Negueruela et al. 2006b).

High-energy observations can give some information about the compact object or about the processes that lead to the emission but do not allow study of the companion star. It is therefore very important to perform multi-wavelength observations of these sources - from optical-to-MIR wavelength - as this represents the only way to characterise the companion or to detect dust around these highly obscured systems. However, positions given by *INTEGRAL* are not accurate enough ($\sim 2'$) to identify their optical counterparts, because of the large number of objects in the error circle. Observations with X-ray telescopes like *XMM-Newton* or *Chandra* are therefore crucial because they allow a localisation with a position accuracy of $4''$ or better, which lowers the number of possible optical counterparts.

We performed optical-to-MIR wavelength observations of several candidate SGXBs recently discovered with *INTEGRAL*. Optical and NIR observations were carried out at ESO/NTT using EMMI and SofI instruments and aimed at constraining the spectral type of the companions through accurate astrometry, as well as the spectroscopy and photometry of the candidate counterparts. They are reported in the companion paper (Chaty et al. 2008, CHA08 hereafter), and it is shown that most of these sources are actually supergiant stars.

In this paper, we report MIR photometric observations of the companions of twelve *INTEGRAL* candidate SFXTs and obscured SGXBs that aimed at studying the circumstellar environment of these highly absorbed sources and, more particularly, at detecting any MIR excess in their emission that could be due to the absorbing material. These sources were chosen because they had very accurate positions and confirmed 2MASS counterparts.

All the sources in our sample are listed in Table 1. The total galactic column density of neutral hydrogen $N_{\text{H}}(\text{H I})$ is computed using the web version of the N_{H} FTOOL from HEASARC. This tool uses the data from Dickey & Lockman

(1990), who performed H I observations from the Lyman- α and 21 cm lines. Moreover, $N_{\text{H}}(\text{H I})$ is the total galactic column density, which means it is integrated along the line of sight over the whole Galaxy. Therefore, it is likely to be overestimated compared to the real value at the distance of the sources.

The total galactic column density of molecular hydrogen $N_{\text{H}}(\text{H}_2)$ is computed using the velocity-integrated map (W_{CO}) and the X-ratio given in Dame, Hartmann, & Thaddeus (2001). It is also likely to be overestimated compared to the real value at the distance of the sources, because it is integrated along the line of sight over the whole Galaxy. In contrast, N_{Hx} , the intrinsic X-ray column density of the source, is computed from the fitting of the high-energy spectral energy distribution (SED), so it takes all the absorption into account at the right distance of the source.

Using these observations, the results reported in the companion paper (CHA08), as well as archival photometric data from the USNO, 2MASS, and GLIMPSE catalogues when needed, we performed the broad-band SEDs of these sources and fitted them with a two-component black body model to assess the contribution of the star and the enshrouding material in the emission. The ESO observations, as well as our model, are described in Section 2. In Section 3, results of the fits for each source are given and these results are discussed in Section 4. We conclude in Section 5.

2. Observations

2.1. MIR observations and data reduction

The MIR observations were carried out on 2005 June 20-22 and 2006 June 29-30 using VISIR (Lagage et al. 2004), the ESO/VLT mid-infrared imager and spectrograph, composed of an imager and a long-slit spectrometer covering several filters in N and Q bands and mounted on Unit 3 of the VLT (Melipal). The standard "chopping and nodding" MIR observational technique was used to suppress the background dominating at these wavelengths. Secondary mirror-chopping was performed in the north-south direction with an amplitude of $16''$ at a frequency of 0.25 Hz. Nodding technique, needed to compensate for chopping residuals, was chosen as parallel to the chopping and applied using telescope offsets of $16''$. Because of the high thermal MIR background for ground-based observations, the detector integration time was set to 16 ms.

We performed broad-band photometry in 3 filters, PAH1 ($\lambda=8.59\pm 0.42 \mu\text{m}$), PAH2 ($\lambda=11.25\pm 0.59 \mu\text{m}$), and Q2 ($\lambda=18.72\pm 0.88 \mu\text{m}$) using the small field in all bands ($19'.2 \times 19'.2$ and $0'.075$ plate scale). All the observations were bracketed with standard star observations for flux calibration and PSF determination. The weather conditions were good and stable during the observations.

Raw data were reduced using the IDL reduction package written by Eric Pantin. The elementary images were co-added in real-time to obtain chopping-corrected data, then the different nodding positions were combined to form the final image. The VISIR detector is affected by stripes randomly triggered by some abnormal high-gain pixels. A dedicated destrip-

ing method was developed (Pantin 2008, in prep.) to suppress them. The MIR fluxes of all observed sources including the 1σ errors are listed in Table 2.

2.2. Archival data

When we did not have optical-to-MIR data for our sources, we searched for the counterparts in 3 catalogues:

- in the United States Naval Observatory (USNO) catalogues in *B*, *R*, and *I* for USNO-B1.0, *B* and *R* for USNO-A.2. Positions and fluxes accuracies are $0''.25$ and 0.3 magnitudes in the case of USNO-B.1, $0''.2$ and 0.5 magnitudes in the case of USNO-A.2.
- in the 2 Micron All Sky Survey (2MASS), in *J* ($1.25 \pm 0.16 \mu\text{m}$), *H* ($1.65 \pm 0.25 \mu\text{m}$) and *Ks* ($2.17 \pm 0.26 \mu\text{m}$) bands. Position accuracy is about $0''.2$.
- in the *Spitzer's* Galactic Legacy Infrared Mid-Plane Survey Extraordinaire (GLIMPSE, Benjamin et al. 2003), survey of the Galactic plane ($|b| \leq 1^\circ$ and between $l=10^\circ$ and $l=65^\circ$ on both sides of the Galactic centre) performed with the *Spitzer Space Telescope*, using the IRAC camera in four bands, $3.6 \pm 0.745 \mu\text{m}$, $4.5 \pm 1.023 \mu\text{m}$, $5.8 \pm 1.450 \mu\text{m}$, and $8 \pm 2.857 \mu\text{m}$.

All sources had a confirmed 2MASS counterpart and three of them (IGR J16195-4945, IGR J16207-5129, and IGR J16318-4848) had a GLIMPSE counterpart given in the literature. We found all the other GLIMPSE counterparts using the 2MASS positions and they are listed in Table 3. We used all the fluxes given in the GLIMPSE catalogue except in the case of IGR J17252-3616, IGR J17391-3021 and IGR J17544-2619 because their fluxes were not present in the catalogue tables. Nevertheless, we measured their fluxes on the archival images directly with aperture photometry. Uncertainties on the measurements were computed in the same way on the error maps given with the data.

2.3. Absorption

Absorption at wavelength λ , A_λ , is a crucial parameter to fit the SEDs, especially in the MIR. Indeed, inappropriate values can lead to a false assessment of the MIR excess. Visible absorption A_V was a free parameter of the fits. An accurate interstellar absorption law - i.e. the wavelength dependence of the $\frac{A_\lambda}{A_V}$ ratio in the line of sight - was then needed to properly fit the SEDs.

In the optical bands, we built the function with the analytical expression given in Cardelli et al. (1989) who derived the average interstellar extinction law in the direction of the Galactic centre. From $1.25 \mu\text{m}$ to $8 \mu\text{m}$, we used the analytical expression given in Indebetouw et al. (2005). They derived it from the measurements of the mean values of the colour excess ratios $\frac{(A_J - A_K)}{(A_J - A_K)}$ from the colour distributions of observed stars in the direction of the Galactic centre. They used archival data from 2MASS and GLIMPSE catalogues, which is relevant in our case as we use GLIMPSE fluxes.

Above $8 \mu\text{m}$, where absorption is dominated by the silicate features at $9.7 \mu\text{m}$ and $18 \mu\text{m}$, we found several extinction laws in the literature (Rieke et al. 1989; Lutz et al. 1996; Moneti et al. 2001), which exhibit some differences. Considering the high importance of a good assessment to correctly fit the MIR excess, we decided to assess the ratio $\frac{A_\lambda}{A_V}$ in 2 VISIR bands - PAH1 and PAH2 - from our data in order to build the relevant law for our observations.

Rieke & Lebofsky (1985) gave the interstellar extinction law up to $13 \mu\text{m}$, and from their results, we derived $0.043 \leq \frac{A_{\text{PAH1}}}{A_V} \leq 0.074$ and $0.047 \leq \frac{A_{\text{PAH2}}}{A_V} \leq 0.06$. To get the best values corresponding to our data in PAH1 and PAH2, we proceeded in 3 steps.

- We first selected the sources for which we had VISIR fluxes in PAH1 and/or PAH2 and fitted their SEDs with extinction laws given in Cardelli et al. (1989) and Indebetouw et al. (2005) from 0.36 to $8 \mu\text{m}$ and half-interval values taken in PAH1 and PAH2.
- Then, when we did not need any MIR excess to fit the IRAC fluxes, we adjusted the $\frac{A_{\text{PAH1}}}{A_V}$ and $\frac{A_{\text{PAH2}}}{A_V}$ ratios to improve the χ^2 of our fits.
- We finally averaged all the extinction values obtained for all sources to get what we consider as the right ratios in PAH1 and PAH2 in the direction of the Galactic plane.

The resulting values are in good agreement with those given by the extinction law from Lutz et al. (1996), so we chose their extinction law to fit our SEDs above $8 \mu\text{m}$, the Q2 filter included. The $\frac{A_\lambda}{A_V}$ values we used in each band are listed in Table 4, and the overall extinction law is displayed in Fig 1.

2.4. SEDs

With all the archival and observational data from optical-to-MIR wavelength, we built the SEDs for these sources. We fitted them (using a χ^2 minimisation) with a model combining two absorbed black bodies, one representing the companion star emission and a spherical one representing a possible MIR excess due to the absorbing material enshrouding the companion star:

$$\lambda F(\lambda) = \frac{2\pi hc^2}{D_*^2 \lambda^4} 10^{-0.4A_\lambda} \left[\frac{R_*^2}{e^{\frac{hc}{\lambda k T_*}} - 1} + \frac{R_D^2}{e^{\frac{hc}{\lambda k T_D}} - 1} \right] \text{ in } \text{W m}^{-2}$$

We added to the flux uncertainties systematic errors as follows:

- a 2% systematic error in each IRAC band as given in the IRAC manual¹
- comparing the variations of the flux calibration values obtained from standards with VISIR during our observation nights, we figured out that systematic errors with VISIR were about 5% at $10 \mu\text{m}$ and 10% at $20 \mu\text{m}$.

¹ <http://ssc.spitzer.caltech.edu/documents/som/som8.0.irac.pdf>

The free parameters of the fits were the absorption in the V-band A_V , the companion star black body temperature T_* and radius to distance ratio $\frac{R_*}{D_*}$, as well as the additional spherical component black body temperature and radius T_D and R_D .

The best-fitting parameters for individual sources, as well as corresponding χ^2 are listed in Table 5 and the fitted SEDs are displayed in Fig 3. Moreover, 90%-confidence ranges of parameters are listed in Table 6.

In Table 5, along with the best-fitting parameters, we also give the total galactic extinctions in magnitudes A_{H1} and A_{H2} in the line of sight, as well as the X-ray extinction of the source in magnitudes A_X . The values of A_{H1} , A_{H2} , and A_X are computed from $N_H(H1)$, $N_H(H2)$, and N_{Hx} given in Table 1 using the relation $A_H = \frac{3.1}{5.8 \times 10^{21} \text{ cm}^{-2}} N_H$ (Bohlin, Savage, & Drake 1978; Rieke & Lebofsky 1985).

3. Results

3.1. IGR J16195-4945

IGR J16195-4945 was detected by *INTEGRAL* during observations carried out between 2003 February 27 and October 19 (Walter et al. 2004) and corresponds to the ASCA source AX J161929-4945 (Sugizaki et al. 2001; Sidoli et al. 2005). Analysing *INTEGRAL* public data, Sidoli et al. (2005) derive an average flux level of ~ 17 mCrab (20-40 keV). Performing a follow-up with *INTEGRAL*, Sguera et al. (2006) show it behaves like an SFXT and report a peak-flux of ~ 35 mCrab (20-40 keV).

Tomsick et al. (2006) observed the source with *Chandra* between 2005 April and July and give its position with $0''.6$ accuracy. They fitted its high-energy emission with an absorbed power law and derive $\Gamma \sim 0.5$ and $N_H \sim 7 \times 10^{22} \text{ cm}^{-2}$. Moreover, using their accurate localisation, they found its NIR and MIR counterparts in the 2MASS (2MASS J16193220-4944305) and in the GLIMPSE (G333.5571+00.3390) catalogues and performed its NIR photometry using ESO/NTT observations. They show its spectral type is compatible with an O, B, or A supergiant star. They also found possible USNO-A.2 and USNO-B.1 counterparts. Nevertheless, as already suggested in their paper, the USNO source is a blended foreground object (Tovmassian et al. 2006).

We observed IGR J16195-4945 on 2006 June 30 in PAH1 during 1200 s, but did not detect it. Typical seeing and airmass were $0''.88$ and 1.07. We nevertheless fitted its SED using the NIR and the GLIMPSE flux values given in Tomsick et al. (2006) and the best-fitting parameters are $A_V=15.5$, $T_*=23800 \text{ K}$, $\frac{R_*}{D_*}=5.96 \times 10^{-11}$, $T_D=1160 \text{ K}$, $R_D=5.1R_*$, and the reduced χ^2 is 3.9/2. The best-fitting parameters without the additional component are $A_V=16.1$, $T_*=13800 \text{ K}$, $\frac{R_*}{D_*}=8.94 \times 10^{-11}$, and the corresponding reduced χ^2 is 15.8/4. We then found a MIR excess.

The additional component is then needed to correctly fit the SED, as this source exhibits a MIR excess. Nevertheless, as shown in Fig 4, this excess is small, and the lack of data above

$8 \mu\text{m}$ does not allow to reach definitive conclusions. Moreover, in both cases (with and without dust), the stellar component is consistent with an O/B supergiant, as already suggested in Tomsick et al. (2006).

3.2. IGR J16207-5129

IGR J16207-5129 is an obscured SGXB that was discovered by *INTEGRAL* during observations carried out between 2003 February 27 and October 19 (Walter et al. 2004).

Tomsick et al. (2006) observed it with *Chandra* during the same run as IGR J16195-4945 and give its position with $0''.6$ accuracy. They also fitted its high-energy emission with an absorbed power law and derive $\Gamma \sim 0.5$ and $N_H \sim 3.7 \times 10^{22} \text{ cm}^{-2}$. Thanks to their accurate localisation, they found its NIR and MIR counterparts in the 2MASS (2MASS J16204627-5130060) and in the GLIMPSE (G333.4590+01.0501) catalogues and performed its NIR photometry using ESO/NTT observations. They show its temperature to be $\geq 18000 \text{ K}$, which indicates the system is an HMXB. They also found its USNO-B1.0 (USNO-B1.0 0384-0560875) counterpart.

We observed IGR J16207-5129 on 2006 June 29 in PAH1 and PAH2 during 1200 s in each filter, and in Q2 during 2400 s. Typical seeing and airmass were $0''.72$ and 1.09. We did not detect it in Q2 but in PAH1 and PAH2. The fluxes we derived are $21.7 \pm 1.4 \text{ mJy}$ and $9.4 \pm 1.3 \text{ mJy}$, respectively.

Using those values, as well as the fluxes from ESO/NTT observations and the GLIMPSE archives found in Tomsick et al. (2006), we fitted its SED, and the best-fitting parameters are $A_V=10.5$, $T_*=33800 \text{ K}$, $\frac{R_*}{D_*}=9.42 \times 10^{-11}$, and the reduced χ^2 is 28.5/9. Negueruela & Schurch (2007) find the spectral type is earlier than B1I; our parameters are therefore in good agreement with their results.

The best fit with the additional component gives a larger reduced χ^2 of 30/7 and $T_D < 200 \text{ K}$, which is not significant, as the presence of such cold material marginally enhances the MIR flux. We therefore think IGR J16207-5129 is an O/B massive star whose enshrouding material marginally contributes to its MIR emission.

3.3. IGR J16318-4848

Main high-energy characteristics of this source can be found in Matt & Guainazzi (2003) and Walter et al. (2003). IGR J16318-4848 was discovered by *INTEGRAL* on 2003 January 29 (Courvoisier et al. 2003) and was then observed with *XMM-Newton*, which allowed a $4''$ localisation. Those observations showed that the source was exhibiting a strong absorption of $N_H \sim 2 \times 10^{24} \text{ cm}^{-2}$, a temperature $kT = 9 \text{ keV}$, and a photon index ~ 2 .

Using this accurate position, Filliatre & Chaty (2004) discovered its optical counterpart and confirmed the NIR counterpart proposed by Walter et al. (2003) (2MASS J16314831-4849005). They also performed photometry and spectroscopy in optical and NIR on 2003 February 23-25 at ESO/NTT and

Table 1. Sample of sources studied in this paper. We give their name, their coordinates (J2000 and galactic), the total galactic column density of neutral hydrogen ($N_{\text{H}}(\text{H I})$) and the total galactic column density of molecular hydrogen ($N_{\text{H}}(\text{H}_2)$) in the line of sight, the X-ray column density of the source (N_{Hx}), their type (SFXT or OBS - obscured sources) and their spectral type (SpT). Their spectral classifications come from optical/NIR spectroscopy, reported in the following references (Ref): c: Chaty et al. (2008), f: Filliatre & Chaty (2004), i: in't Zand et al. (2006), n1: Negueruela et al. (2005), n2: Negueruela et al. (2006a), n3: Nespoli et al. (2007), p: Pellizza et al. (2006), t: Tomsick et al. (2006).

Sources	α (J2000)	δ (J2000)	l	b	$N_{\text{H}}(\text{H I})(10^{22})$	$N_{\text{H}}(\text{H}_2)(10^{22})$	$N_{\text{Hx}}(10^{22})$	Type	SpT	Ref
IGR J16195-4945	16 19 32.20	-49 44 30.7	333.56	0.339	2.2	5.4	7.0	SFXT ?	O/B	t
IGR J16207-5129	16 20 46.26	-51 30 06.0	332.46	-1.050	1.7	2.2	3.7	OBS	O/B	t
IGR J16318-4848	16 31 48.60	-48 49 00.0	335.62	-0.448	2.1	3.6	200.0	OBS	sgB[e]	f
IGR J16320-4751	16 32 01.90	-47 52 27.0	336.30	0.169	2.1	4.4	21.0	OBS	O/BI	c
IGR J16358-4726	16 35 53.80	-47 25 41.1	337.01	-0.007	2.2	7.3	33.0	OBS	sgB[e]	c
IGR J16418-4532	16 41 51.00	-45 32 25.0	339.19	0.489	1.9	3.6	10.0	SFXT ?	O/B	c
IGR J16465-4507	16 46 35.50	-45 07 04.0	340.05	0.135	2.1	5.9	60.0	SFXT	B0.5I	n1
IGR J16479-4514	16 48 06.60	-45 12 08.0	340.16	-0.124	2.1	8.2	7.7	SFXT ?	O/BI	c
IGR J17252-3616	17 25 11.40	-36 16 58.6	351.50	-0.354	1.6	3.9	15.0	OBS	O/BI	c
IGR J17391-3021	17 39 11.58	-30 20 37.6	358.07	0.445	1.4	4.5	30.0	SFXT	08Iab(f)	n2
IGR J17544-2619	17 54 25.28	-26 19 52.6	3.26	-0.336	1.4	7.8	1.4	SFXT	O9Ib	p
IGR J19140+0951	19 14 04.23	+09 52 58.3	44.30	-0.469	1.7	3.7	6.0	OBS	BII	n3

Table 2. Summary of VISIR observations of newly discovered *INTEGRAL* sources. We give their MIR fluxes (mJy) in the PAH1 (8.59 μm), PAH2 (11.25 μm) and Q2 (18.72 μm) filters. When we did not detect a source, we give the upper limit. When no flux nor upper limit is given, the source was not observed in the considered filter.

Sources	PAH1	PAH2	Q2
IGR J16195-4945	< 6.1	< 7.8	< 50.3
IGR J16207-5129	21.7 \pm 1.4	9.4 \pm 1.3	< 53.4
IGR J16318-4848	426.2 \pm 3.0	317.4 \pm 3.4	180.7 \pm 15.3
IGR J16320-4751	12.1 \pm 1.7	6.3 \pm 1.8	
IGR J16358-4726	< 6.9		
IGR J16418-4532	< 5.8		
IGR J16465-4507	6.9 \pm 1.1	< 5.0	
IGR J16479-4514	10.9 \pm 1.2	7.0 \pm 1.6	
IGR J17252-3616	6.1 \pm 0.6	< 5.0	
IGR J17391-3021	70.2 \pm 1.6	46.5 \pm 2.6	
IGR J17544-2619	46.1 \pm 2.8	20.2 \pm 2.1	
IGR J19140+0951	35.2 \pm 1.4	19.1 \pm 1.4	

show that the source presents a significant NIR excess and that it is strongly absorbed ($A_{\text{V}} \sim 17.4$). The spectroscopy revealed an unusual spectrum with a continuum very rich in strong emission lines, which, together with the presence of forbidden lines, points towards an sgB[e] companion star (see e.g. Lamers et al. 1998; Zickgraf 1999, for definition and characteristics of these stars).

Using the 2MASS magnitudes, the GLIMPSE (G335.6260-00.4477), and the MSX fluxes, Kaplan et al. (2006) fitted its SED with a combination of a stellar and a dust component black bodies, and shows that the presence of warm dust around the system was necessary for explaining the NIR and MIR excess. From their fit, they derive $A_{\text{V}} \sim 18.5$, $T_{\text{D}}=1030$ K, and $R_{\text{D}}=10R_{\odot}$.

- the first time on 2005 June 21 during 300 s in PAH1 and PAH2, and 600 s in Q2. Typical seeing and airmass were 0'81 and 1.14. We detected the source in all bands, and the derived fluxes are 409.2 \pm 2.4 mJy, 322.4 \pm 3.3 mJy, and 172.1 \pm 14.9 mJy in PAH1, PAH2, and Q2, respectively.
- the second on 2006 June 30 during 600 s in all bands. Typical seeing and airmass were 0'68 and 1.09. We detected the source in all bands, and the derived fluxes are 426.2 \pm 3.0 mJy, 317.4 \pm 3.4 mJy, and 180.7 \pm 15.3 mJy in PAH1, PAH2, and Q2, respectively.

Those observations show that IGR J16318-4848 is very bright in the MIR (it is actually the brightest source in our sample) and that its flux was constant within a year, considering VISIR systematic errors.

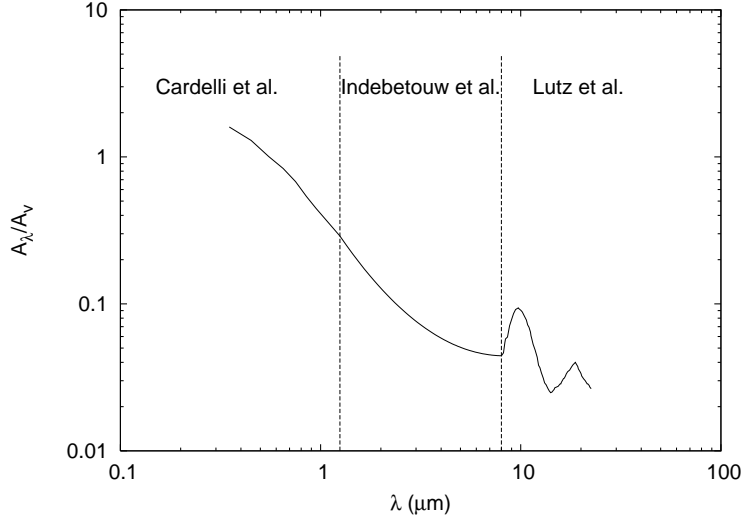
Using data from our last run, as well as the magnitudes given in Filliatre & Chaty (2004) in the optical and the NIR, and the fluxes from the GLIMPSE archives, we fitted its

Table 3. List of GLIMPSE counterparts we found for 9 sources. We give their name, their separation from the 2MASS counterparts and their fluxes in mJy.

Sources	GLIMPSE counterpart	Separation	3.6 μm	4.5 μm	5.8 μm	8 μm
IGR J16320-4751	G336.3293+00.1689	0'17	48.2 \pm 1.9	44.3 \pm 2.1	36.0 \pm 2.0	17.3 \pm 1.0
IGR J16358-4726	G337.0994-00.0062	0'46	5.9 \pm 0.5	5.6 \pm 0.6	5.3 \pm 1.7	
IGR J16418-4532	G339.1889+00.4889	0'28	12.5 \pm 0.9	9.5 \pm 0.6	5.6 \pm 0.6	3.6 \pm 0.4
IGR J16465-4507	G340.0536+00.1350	0'16	45.0 \pm 2.0	32.6 \pm 1.5	22.0 \pm 0.9	13.7 \pm 0.6
IGR J16479-4514	G340.1630-00.1239	0'13	68.6 \pm 3.1	49.6 \pm 2.0	41.2 \pm 2.3	19.4 \pm 0.9
IGR J17252-3616			32.6 \pm 3.7	24.7 \pm 4.7	21.8 \pm 5.0	9.6 \pm 6.5
IGR J17391-3021			375.9 \pm 44.0	297.0 \pm 31.0	205.0 \pm 33.0	111.0 \pm 28.0
IGR J17544-2619			213.9 \pm 25.4	137.0 \pm 18.9	99.6 \pm 7.6	66.5 \pm 12.1
IGR J19140+0951	G044.2963-00.4688	0'48	185.0 \pm 9.3	152.0 \pm 11.1	103.9 \pm 5.4	62.0 \pm 2.1

Table 4. Adopted $\frac{A_\lambda}{A_V}$ values.

Filters	<i>U</i>	<i>B</i>	<i>V</i>	<i>R</i>	<i>I</i>	<i>J</i>	<i>H</i>	<i>Ks</i>	3.6 μm	4.5 μm	5.8 μm	8 μm	8.59 μm	11.25 μm	18.72 μm
$\frac{A_\lambda}{A_V}$	1.575	1.332	1	0.757	0.486	0.289	0.174	0.115	0.0638	0.0539	0.0474	0.0444	0.0595	0.0605	0.040

**Fig. 1.** Adopted extinction law. We used the law given in Cardelli et al. (1989) in the optical, the one given in Indebetouw et al. (2005) from 1.25 μm to 8 μm , and the law from Lutz et al. (1996) above 8 μm .

SED and the best-fitting parameters are $A_V=17$, $T_*=22200$ K, $\frac{R_*}{D_*}=3.74 \times 10^{-10}$, $T_D=1100$ K, $R_D=10R_*$, and the reduced χ^2 is 6.6/6. The best-fitting parameters without the additional component are $A_V=17.9$, $T_*=18200$ K, $\frac{R_*}{D_*}=5.1 \times 10^{-10}$, and the corresponding reduced χ^2 is 425/8. We then confirm that the MIR excess is likely due to the presence of warm dust around the system, as already suggested by Filliatre & Chaty (2004) and reported in Kaplan et al. (2006).

3.4. IGR J16320-4751

IGR J16320-4751 was detected by *INTEGRAL* on 2003 February (Tomsick et al. 2003) and corresponds to the ASCA source AX J1631.9-4752. Rodriguez et al. (2003) report observations with *XMM-Newton*. They give an accurate localisa-

tion (3'') and fitted its high-energy spectrum with an absorbed power law. They derive $\Gamma \sim 1.6$ and $N_H \sim 2.1 \times 10^{23} \text{ cm}^{-2}$.

Lutovinov et al. (2005) report the discovery of X-Ray pulsations ($P \sim 1309$ s), which proves the compact object is a neutron star. Moreover, Corbet et al. (2004) obtained the light curve of IGR J16320-4751 between 2004 December 21 and 2005 September 17 with Swift and report the discovery of a 8.96 days orbital period. IGR J16320-4751 is then an X-ray binary whose compact object is a neutron star.

Negueruela & Schurch (2007) searched for the NIR counterpart of the source in the 2MASS catalogue and found its position was consistent with 2MASS J16320215-4752289. They also concluded that, if it was an O/B supergiant, it had to be extremely absorbed.

The optical and NIR photometry and spectroscopy of this source were carried out at ESO/NTT, and results are reported

Table 5. Summary of best-fitting parameters of the SEDs of the sources. We give the total galactic extinctions in magnitudes A_{H1} and A_{H2} , the X-ray extinction of the source in magnitudes A_X and then the parameters themselves: the extinction in the optical A_V , the temperature T_* and the $\frac{R_c}{D_*}$ ratio of the companion and the temperature and radius T_D and R_D (in R_* unit) of the dust component when needed. We also add the reduced χ^2 we reach for each fit.

Sources	A_{H1}	A_{H2}	A_X	A_V	$T_*(K)$	$\frac{R_c}{D_*}$	$T_D(K)$	$R_D(R_*)$	χ^2/dof
IGR J16195-4945	11.7	28.6	37.4	15.5	23800	5.96×10^{-11}	1160	5.1	3.9/2
IGR J16207-5129	9.3	11.8	19.8	10.5	33800	9.42×10^{-11}			28.5/9
IGR J16318-4848	11.0	19.2	1069.5	17.0	22200	3.74×10^{-10}	1100	10.0	6.6/6
IGR J16320-4751	11.4	23.6	112.2	35.4	33000	1.38×10^{-10}			7.7/6
IGR J16358-4726	11.8	39.4	176.4	17.6	24500	3.16×10^{-11}	810	10.1	3.6/2
IGR J16418-4532	10.1	19.3	53.5	14.5	32800	3.77×10^{-11}			1.4/4
IGR J16465-4507	11.3	31.4	320.7	5.9	25000	6.40×10^{-11}			13.9/7
IGR J16479-4514	11.4	43.8	41.2	18.5	32800	1.00×10^{-10}			7.4/6
IGR J17252-3616	8.3	20.1	80.2	20.8	32600	7.57×10^{-11}			3.8/5
IGR J17391-3021	7.3	23.9	160.4	9.2	31400	1.80×10^{-10}			11.7/10
IGR J17544-2619	7.7	41.5	7.70	6.1	31000	1.27×10^{-10}			6.1/8
IGR J19140+0951	9.0	14.0	32.1	16.5	22500	1.92×10^{-10}			14.4/6

Table 6. Ranges of parameters that give acceptable fits (90%-confidence) for each source.

Sources	ΔA_V	ΔT_*	$\Delta \frac{R_c}{D_*}$	ΔT_D	ΔR_D
IGR J16195-4945	14.8 – 15.8	13100 – 25900	$5.68 \times 10^{-11} - 6.68 \times 10^{-11}$	950 – 1460	3.9 – 6.6
IGR J16207-5129	10.4 – 10.6	25200 – 36000	$9.36 \times 10^{-11} - 1.05 \times 10^{-10}$		
IGR J16318-4848	16.6 – 17.4	19300 – 24500	$3.65 \times 10^{-10} - 3.84 \times 10^{-10}$	960 – 1260	8.8 – 11.8
IGR J16320-4751	34.8 – 35.5	22000 – 35600	$1.33 \times 10^{-10} - 1.69 \times 10^{-10}$		
IGR J16358-4726	17.1 – 18.1	19500 – 36000	$2.64 \times 10^{-11} - 3.52 \times 10^{-11}$	630 – 1020	8.0 – 13.8
IGR J16418-4532	13.6 – 14.7	10600 – 36000	$3.58 \times 10^{-11} - 5.44 \times 10^{-11}$		
IGR J16465-4507	5.0 – 6.1	15400 – 33600	$5.50 \times 10^{-11} - 7.95 \times 10^{-11}$		
IGR J16479-4514	18.4 – 18.8	26200 – 36000	$9.48 \times 10^{-11} - 1.13 \times 10^{-10}$		
IGR J17252-3616	20.3 – 21.0	20500 – 36000	$7.17 \times 10^{-11} - 9.48 \times 10^{-11}$		
IGR J17391-3021	8.8 – 9.4	16100 – 32200	$1.78 \times 10^{-10} - 2.63 \times 10^{-10}$		
IGR J17544-2619	6.0 – 6.2	26700 – 35500	$1.18 \times 10^{-10} - 1.38 \times 10^{-10}$		
IGR J19140+0951	15.7 – 16.7	13200 – 28100	$1.71 \times 10^{-10} - 2.53 \times 10^{-10}$		

in CHA08. It is shown that its NIR spectrum is consistent with an O/B supergiant and that its intrinsic absorption is very high, because it was not detected in any of the visible bands. We searched for the MIR counterpart of IGR J16320-4751 in the GLIMPSE archives and found it to be consistent with G336.3293+00.1689.

We observed IGR J16320-4751 with VISIR on 2005 June 20 in PAH1 and PAH2, and the respective exposure times were 1800 s and 2400 s. Typical seeing and airmass were $0''.63$ and 1.13. We detected it in both filters, and the respective fluxes are 12.1 ± 1.7 mJy and 6.3 ± 1.8 mJy. Using the ESO/NTT NIR magnitudes given in CHA08, as well as the GLIMPSE and the VISIR fluxes, we fitted its SED and the best-fitting parameters are $A_V=35.4$, $T_*=33000$ K, $\frac{R_c}{D_*}=1.38 \times 10^{-10}$, and the reduced χ^2 is 7.7/6. This result is in good agreement with an extremely absorbed O/B supergiant as reported in CHA08.

The best fit with the additional component gives a larger reduced χ^2 of 8/4 and $T_D < 200$ K. We therefore think that

IGR J16320-4751 is an O/B supergiant whose enshrouding material marginally contributes to its MIR emission, even if its intrinsic absorption is extremely high.

3.5. IGR J16358-4726

IGR J16358-4726 was detected with *INTEGRAL* on 2003 March 19 (Revnivtsev et al. 2003) and first observed with *Chandra* on 2003 March 24 (Patel et al. 2004). They give its position with $0''.6$ accuracy and fitted its high-energy spectrum with an absorbed power law. They derive $\Gamma \sim 0.5$ and $N_H \sim 3.3 \times 10^{23} \text{ cm}^{-2}$. They also found a 5880 ± 50 s modulation, which could be either a neutron star pulsation or an orbital modulation. Nevertheless, Patel et al. (2006) performed detailed spectral and timing analysis of this source using multi-satellite archival observations and identified a 94 s spin up, which points to a neutron star origin. Assuming that this spin up was due to accretion, they estimate the source magnetic field is between 10^{13} and 10^{15} G, which could support a magnetar nature for IGR J16358-4726.

Kouveliotou et al. (2003) propose 2MASS J16355369-4725398 as the possible NIR counterpart, and NIR spectroscopy and photometry of this counterpart was performed at ESO/NTT and is reported in CHA08. They show that its spectrum is consistent with a B supergiant belonging to the same family as IGR J16318-4848, the so-called B[e] supergiants. We also found its MIR counterpart in the GLIMPSE archives (G337.0994-00.0062).

We observed IGR J16358-4726 with VISIR on 2006 June 29 but did not detect it in any filter. Using the NIR magnitudes given in CHA08 and the GLIMPSE fluxes, we fitted its SED and the best-fitting parameters are $A_V=17.6$, $T_*=24500$ K, $\frac{R_*}{D_*}=3.16 \times 10^{-11}$, $T_D=810$ K, $R_D=10.1R_*$, and the reduced χ^2 is 3.6/2. The best-fitting parameters without the additional component are $A_V=16.7$, $T_*=9800$ K, $\frac{R_*}{D_*}=6.05 \times 10^{-11}$ and the corresponding reduced χ^2 is 8.8/4.

The additional component is then necessary to correctly fit the SED, since this source exhibits a MIR excess (see Fig 4). Even if we lack MIR data above $5.8 \mu\text{m}$, we think this excess is real and stems from warm dust, as it is consistent with the source being a sgB[e], as reported in CHA08.

3.6. IGR J16418-4532

IGR J16418-4532 was discovered with *INTEGRAL* on 2003 February 1-5 (Tomsick et al. 2004). Using *INTEGRAL* observations, Sguera et al. (2006) report an SFXT behaviour of this source and a peak-flux of ~ 80 mCrab (20-30 keV). Moreover, using *XMM-Newton* and *INTEGRAL* observations, Walter et al. (2006) report a pulse period of 1246 ± 100 s and derive $N_H \sim 10^{23} \text{ cm}^{-2}$. They also proposed 2MASS J16415078-4532253 as its likely NIR counterpart. The NIR photometry of this counterpart was performed at ESO/NTT and is reported in CHA08. We also found the MIR counterpart in the GLIMPSE archives (G339.1889+004889).

We observed IGR J16418-4532 with VISIR on 2006 June 29 but did not detect it in any filter. Using The NIR magnitudes given in CHA08, as well as the GLIMPSE fluxes, we fitted its SED, and the best-fitting parameters are $A_V=14.5$, $T_*=32800$ K, $\frac{R_*}{D_*}=3.77 \times 10^{-11}$, and the reduced χ^2 is 1.4/4. The best fit with the additional component gives a larger reduced χ^2 of 3.9/2 and $T_D < 200$ K.

Uncertainties on the data are high, which is the reason why the reduced χ^2 are low. Nevertheless, parameters of the fit, as well as the 90%-confidence ranges of parameters listed in Table 6, are consistent with an O/B massive star nature. The temperature of the additional component being insignificant, we conclude this source is an O/B massive star whose enshrouding material marginally contributes to its MIR emission.

3.7. IGR J16465-4507

IGR J16465-4507 is a transient source discovered with *INTEGRAL* on 2004 September 6-7 (Lutovinov et al. 2004).

Observations were carried out on 2004 September 14 with *XMM-Newton*, and Zurita Heras & Walter (2004) report a position with $4''$ accuracy, allowing identification of an NIR counterpart in the 2MASS catalogue (2MASS J16463526-4507045=USNO-B1.0 0448-00520455). With the ESO/NTT, Negueruela et al. (2005) performed intermediate-resolution spectroscopy of the source, estimate the spectral type is a B0.5I, and propose that it is an SFXT. Using *XMM-Newton* and *INTEGRAL*, Walter et al. (2006) find a pulse period of 227 ± 5 s and derive $N_H \sim 6 \times 10^{23} \text{ cm}^{-2}$. We found its MIR counterpart in the GLIMPSE archives (G340.0536+00.1350) using the 2MASS position.

We observed IGR J16465-4507 with VISIR twice:

- The first one on 2005 June 20 during 600 s in PAH1. Typical seeing and airmass were $0''.81$ and 1.14. We detected the source and the derived flux is 8.7 ± 1.8 mJy.
- the second on 2006 June 30 during 1200 s in PAH1 and PAH2. Typical seeing and airmass were $0''.68$ and 1.09. We detected the source in PAH1 but not in PAH2. The derived flux is 6.9 ± 1.1 mJy.

These observations show that the IGR J16465-4507 MIR flux was constant during the year.

Using the USNO-B1.0, 2MASS, and GLIMPSE flux values, as well as our VISIR data, we fitted its SED, and the best-fitting parameters are $A_V=5.9$, $T_*=25000$ K, $\frac{R_*}{D_*}=6.4 \times 10^{-11}$, and the reduced χ^2 is 13.9/7. The best fit with the additional components gives a larger reduced χ^2 of 20/5 and $T_D < 200$ K.

We then conclude that no additional component is needed to explain the MIR emission of this source, and the parameters derived from our fit are in good agreement with IGR J16465-4507 being a B0.5I as reported in Negueruela et al. (2005).

3.8. IGR J16479-4514

IGR J16479-4514 was discovered with *INTEGRAL* on 2003 August 8-9 (Molkov et al. 2003). Sguera et al. (2005) suggest it is a fast transient after they detected recurrent outbursts, and Sguera et al. (2006) report a peak-flux of ~ 120 mCrab (20-60 keV). Walter et al. (2006) observed it with *XMM-Newton* and gave its position with $4''$ accuracy. Moreover, they derive $N_H \sim 7.7 \times 10^{22} \text{ cm}^{-2}$ from their observations. They also propose 2MASS J16480656-4512068=USNO-B1.0 0447-0531332 as its likely NIR counterpart. The NIR spectroscopy and photometry of this counterpart were performed at ESO/NTT and are reported in CHA08. It is shown that its spectrum is consistent with an O/B supergiant. We also found the MIR counterpart in the GLIMPSE archive (G339.1889+004889).

We observed IGR J16479-4514 with VISIR on 2006 June 29 in PAH1 and PAH2, and the exposure time was 1200 s in each filter. Typical seeing and airmass were $0''.9$ and 1.14. We detected it in both filters, and the respective fluxes are 10.9 ± 1.2 mJy and 7.0 ± 1.6 mJy. Using the NIR magnitudes

given in CHA08, as well as the GLIMPSE and the VISIR fluxes, we fitted its SED, and the best-fitting parameters are $A_V=18.5$, $T_*=32800$ K, $\frac{R_*}{D_*}=1.00 \times 10^{-10}$, and the reduced χ^2 is 7.4/6. The best fit with the additional component gives a larger reduced χ^2 of 9/4 and $T_D < 200$ K.

We then do not need any additional component to fit the SED, and our result is consistent with IGR J16479-4514 being an obscured O/B supergiant, in good agreement with CHA08.

3.9. IGR J17252-3616

IGR J17252-3616 is a heavily-absorbed persistent source discovered with *INTEGRAL* on 2004 February 9 and reported in Walter et al. (2004). It was observed with *XMM-Newton* on 2004 March 21, and Zurita Heras et al. (2006) give its position with 4'' accuracy. Using the *XMM-Newton* observations, as well as those carried out with *INTEGRAL*, they show the source was a binary X-ray pulsar with a spin period of ~ 413.7 s and an orbital period of ~ 9.72 days, and derive $N_H \sim 1.5 \times 10^{23}$ cm $^{-2}$. Moreover, they fitted its high-energy spectrum with either an absorbed compton (kT ~ 5.5 keV and $\tau \sim 7.8$) or a flat power law ($\Gamma \sim 0.02$).

In their paper, they propose 2MASS J17251139-3616575 as its likely NIR counterpart, as do Negueruela & Schurch (2007). The NIR spectroscopy and photometry of this counterpart were performed at ESO/NTT and are reported in CHA08, where it is shown that its spectrum is consistent with an O/B supergiant. Using the 2MASS position, we searched for its MIR counterpart in the GLIMPSE catalogue. Unfortunately, we did not find its IRAC fluxes in the database. Nevertheless, we found post-Basic Calibrated Data (post-BCD) images of the source in all filters. We then reduced those data and derived fluxes directly from the images. They are listed in Table 3.

We observed IGR J17252-3616 with VISIR on 2006 June 30 in PAH1 and PAH2 and the exposure time was 1200 s in each filter. Typical seeing and airmass were 0''.97 and 1.09. We detected it in PAH1, and the derived flux is 6.1 ± 0.6 mJy. Using the NIR magnitudes given in CHA08, as well as the GLIMPSE and the VISIR fluxes, we fitted its SED, and the best-fitting parameters are $A_V=20.8$, $T_*=32600$ K, $\frac{R_*}{D_*}=7.57 \times 10^{-11}$, and the reduced χ^2 is 3.8/5. The best fit with the additional component gives a larger reduced χ^2 of 6.9/3 and $T_D < 200$ K. We then do not need any additional component to fit the SED, and our result is consistent with IGR J17252-3616 to be an obscured O/B supergiant, in good agreement with CHA08.

3.10. IGR J17391-3021

IGR J17391-3021 is a transient source discovered with *INTEGRAL* on 2003 August 26 (Sunyaev et al. 2003) and it corresponds to the *Rossi X-ray Timing Explorer (RXTE)* source XTE J1739-302. Sguera et al. (2005) analysed archival *INTEGRAL* data and classified the source as a fast X-ray transient presenting a typical neutron star spectrum. Smith et al. (2006) observed it with *Chandra* on 2003 October 15 and give its precise position with 1'' accuracy. They

also give its optical/NIR counterpart 2MASS J17391155-3020380=USNO-B1.0 0596-0585865 and classify IGR J17391-3021 as an SFXT. Negueruela et al. (2006a) performed optical/NIR photometry and spectroscopy of the companion using ESO/NTT and find it is a O8Iab(f) star whose distance is ~ 2.3 kpc. CHA08 also report optical and NIR spectroscopy and photometry of the companion carried out at ESO/NTT and confirm the nature of the companion. Using the 2MASS position, we searched for its MIR counterpart in the GLIMPSE catalogue and as for IGR J17252-3616, we had to reduce post-BCD data and derive the fluxes directly from the images. The fluxes are listed in Table 3.

We observed IGR J17391-3021 with VISIR on 2005 June 20 in PAH1 and PAH2, and the exposure time was 600 s in each filter. Typical seeing and airmass were 0''.63 and 1.13. We detected it in both filters, and the derived fluxes are 70.2 ± 1.6 mJy and 46.5 ± 2.6 mJy. Using the optical and the NIR magnitudes given in CHA08, as well as the GLIMPSE and the VISIR fluxes, we fitted its SED and the best-fitting parameters are $A_V=9.2$, $T_*=31400$ K, $\frac{R_*}{D_*}=1.8 \times 10^{-10}$, and the reduced χ^2 is 11.7/10. The best fit with the additional component gives a larger reduced χ^2 of 15.3/8 and $T_D < 200$ K.

We then do not need any additional component to fit the SED, and the parameters derived from our fit are in good agreement with IGR J17391-3021 to be an O8Iab(f) supergiant star, as initially reported in Negueruela et al. (2006a).

3.11. IGR J17544-2619

IGR J17544-2619 is a transient source discovered with *INTEGRAL* on 2003 September 17 (Sunyaev et al. 2003). González-Riestra et al. (2004) observed it with *XMM-Newton* and derive $N_H \sim 2 \times 10^{22}$ cm $^{-2}$. They also confirm the association of the companion with 2MASS J17542527-2619526=USNO-B1.0 0636-0620933, as proposed in Rodriguez (2003). in't Zand (2005) report on observations performed with *Chandra*, give its position with 0''.6 accuracy, $N_H \sim 1.36 \times 10^{22}$ cm $^{-2}$, and show that its high-energy spectrum is typical of an accreting neutron star. Moreover, they identify the counterpart as a blue supergiant. Sguera et al. (2006) report a peak-flux of ~ 240 mCrab. Using ESO/NTT, Pellizza et al. (2006) performed optical/NIR spectroscopy and photometry of the companion, and give its spectral type as O9Ib at 2.1-4.2 kpc. Using the 2MASS position, we searched for its MIR counterpart in the GLIMPSE catalogue, and as for IGR J17252-3616 and IGR J17391-3021, we had to reduce post-BCD data and derived the fluxes directly from the images. The fluxes are listed in Table 3.

We observed IGR J17544-2619 with VISIR on 2005 June 20 in PAH1 and PAH2, and the exposure time was 600 s in PAH1 and 1200 s in PAH2. Typical seeing and airmass were 0''.64 and 1.13. We detected it in both filters, and the derived fluxes are 46.1 ± 2.8 mJy and 20.2 ± 2.1 mJy. Using the magnitudes from Pellizza et al. (2006), the GLIMPSE and the VISIR fluxes, we fitted its SED, and the best-fitting parameters are

$A_V=6.1$, $T_*=31000$ K, $\frac{R_*}{D_*}=1.27 \times 10^{-10}$, and the reduced χ^2 is 6.1/8. The best fit with the additional component gives a larger reduced χ^2 of 9/6 and $T_D < 200$ K.

We then do not need any additional component to fit the SED, and the parameters derived from our fit are in good agreement with IGR J17544-2619 as an O9Ib supergiant star, as initially reported in Pellizza et al. (2006).

3.12. IGR J19140+0951

IGR J19140+0951 is a persistent source that was discovered with *INTEGRAL* on 2003 March 6-7 (Hannikainen et al. 2003). Observations carried out with *RXTE* allowed $\Gamma \sim 1.6$ and $N_H \sim 6 \times 10^{22} \text{ cm}^{-2}$ to be derived (Swank & Markwardt 2003). Timing analysis of the *RXTE* data showed a period of 13.55 days (Corbet et al. 2004), which shows the binary nature of the source. After a comprehensive analysis of *INTEGRAL* and *RXTE* data, Rodriguez et al. (2005) show the source is spending most of its time in a faint state but report high variations in luminosity and absorption column density (up to $\sim 10^{23} \text{ cm}^{-2}$). They also find evidence that the compact object is a neutron star rather than a black hole. Using *Chandra* observations carried out 2004 May 11, in't Zand et al. (2006) give its position with $0''.6$ accuracy. This allowed them to find its NIR counterpart in the 2MASS catalogue (2MASS J19140422+0952577). Moreover, they searched for its MIR counterpart in the Mid-course Space Experiment (MSX Mill 1994) and found an object at $8.3 \mu\text{m}$. The NIR photometry and spectroscopy of this source were performed at ESO/NTT and results are reported in CHA08. It is shown that its spectrum is consistent with an O/B massive star, in good agreement with Nespoli et al. (2007), who show it is a B1I supergiant. Using the 2MASS position, we also found its MIR counterpart in the GLIMPSE archive (G044.2963-00.4688).

We observed IGR J19140+0951 with VISIR on 2006 June 30 in PAH1 and PAH2, and the exposure time was 1200 s in each filter. Typical seeing and airmass were $1''.12$ and 1.17. We detected it in both filters, and the derived fluxes are 35.2 ± 1.4 mJy and 19.1 ± 1.4 mJy. We point out that the object given as the MSX counterpart of IGR J19140+0951 in in't Zand et al. (2006) is a blended source. Indeed, VISIR images, whose resolution is far better, clearly show there are two sources in the field, IGR J19140+0951 and a very bright southern source (see Fig 2).

Using the magnitudes given in CHA08, as well as the fluxes from GLIMPSE and our observations with VISIR, we fitted its SED, and the best-fitting parameters are $A_V=16.5$, $T_*=22500$ K, $\frac{R_*}{D_*}=1.92 \times 10^{-10}$, and the reduced χ^2 is 14.4/6. The best fit with the additional component gives a larger reduced χ^2 of 20.2/4 and $T_D < 200$ K.

We do not need any additional component to fit the SED, and the parameters derived from our fit are in good agreement with IGR J19140+0951 to be an B1I supergiant star, as initially reported in Nespoli et al. (2007).

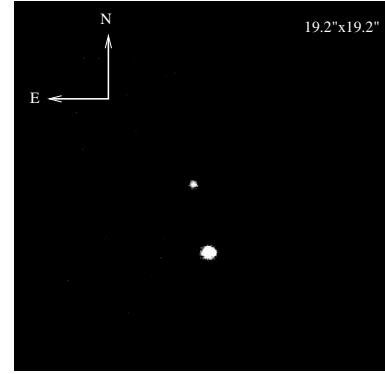


Fig. 2. VISIR image of IGR J19140+0951 in PAH1 ($8.59 \mu\text{m}$). $19.2'' \times 19.2''$ field of view and $0''.075$ plate scale. We clearly see the two sources that were blended with MSX. The MIR counterpart of IGR J19140+0951 is the northern source.

4. Discussion

4.1. B vs B[e] supergiants stellar winds

All SEDs were best-fitted without any dust component (even the very absorbed one like IGR J16320-4751), except three of them (IGR J16195-4945, IGR J16318-4848, and IGR J16358-4726, see Fig. 3) that exhibit a MIR excess likely due to the presence of dust in their stellar wind.

Blue supergiants are known to exhibit a very strong but sparse stellar wind of high velocity ($\sim 1000\text{-}2000 \text{ km s}^{-1}$). This has been explained through the so-called radiation line-driven CAK model (Castor, Abbott, & Klein 1975) in which the wind is driven by absorption in spectral lines. Hot stars emit most of their radiation in the ultraviolet (UV) where their atmosphere has many absorption lines. Photons coming from the photosphere of the star with the same wavelength are absorbed and re-emitted to the expanding medium in a random direction with almost the same momentum, which results in acceleration of the wind. This process is very effective because the line spectrum of the scattering ions in the wind is Doppler-shifted compared to the stellar rest frame, so the scattering atoms are shifted with respect to their neighbours at lower velocities and can interact with an unaffected part of the stellar spectrum.

IGR J16318-4848 was proven to belong to a particular class of B1 supergiants, the B[e] supergiants or sgB[e] (Filliatre & Chaty 2004). A physical definition of B[e] stars can be found in Lamers et al. (1998). We just recall two of the characteristics here: the presence of forbidden emission lines of [Fe II] and [O I] in the NIR spectrum and of a strong MIR excess due to hot circumstellar dust that re-emits the absorbed stellar radiation through free-free emission. An sgB[e] is defined by the B[e] phenomenon, the indication of mass-loss in the optical spectrum (P-cygni profiles), and a hybrid spectrum characterised by the simultaneous presence of narrow low-excitation lines and broad absorption features of high-excitation lines. This hybrid nature was empirically explained by the simultaneous presence of a normal supergiant hot polar wind (fast and sparse) and responsible for the broad

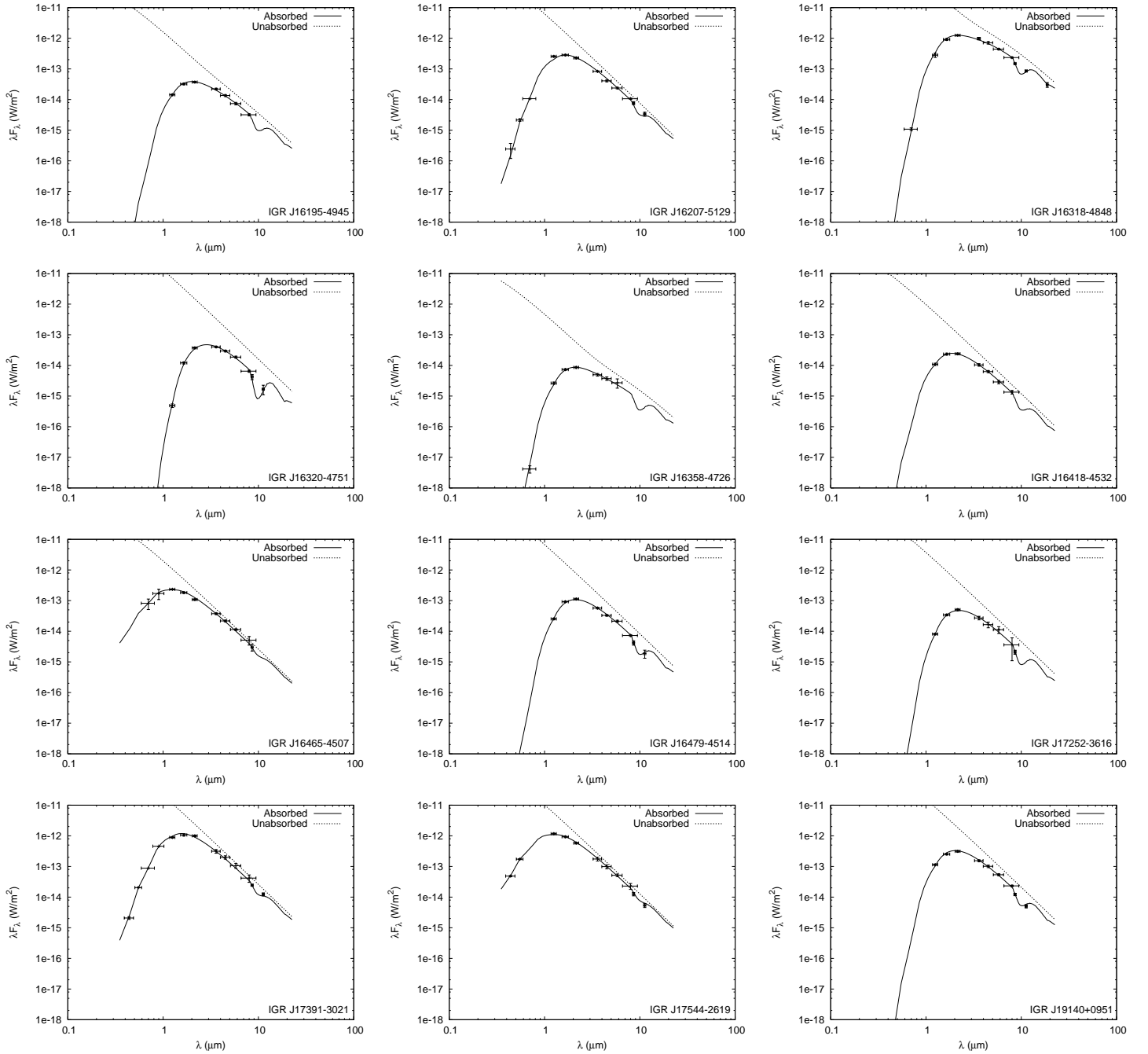


Fig. 3. Optical-to-MIR absorbed (line) and unabsorbed (dotted-line) SEDs of 12 *INTEGRAL* sources, including broad-band photometric data from ESO/NTT, 2MASS, GLIMPSE, and VISIR.

lines and a cool equatorial outflowing disk-like wind (slow and dense) responsible for the narrow lines (Shore & Sanduleak 1983; Zickgraf et al. 1985; Shore et al. 1987). This empirical model has received some confirmation from polarimetry (Oudmaijer & Drew 1999).

There are a few models that explain the creation of this outflowing disk, and all of them consider the star rotation to be an important parameter in the process. In this paper, we present only the most consistent of them, the Rotation Induced Bi-stability mechanism (RIB), but a review can be found in

Kraus & Miroshnichenko (2006).

The lines responsible for the creation of the wind are dependent on the ionisation structure, and a change in this structure leads to a change in the radiative flux. This is the bi-stability jump found by Lamers & Pauldrach (1991), which appears for B stars with effective temperatures of about 23000 K. Above this temperature, the wind tends to be fast and sparse. Below, the mass-loss rate is five times higher and the terminal velocity two times slower, which leads to a wind that is ten times denser.

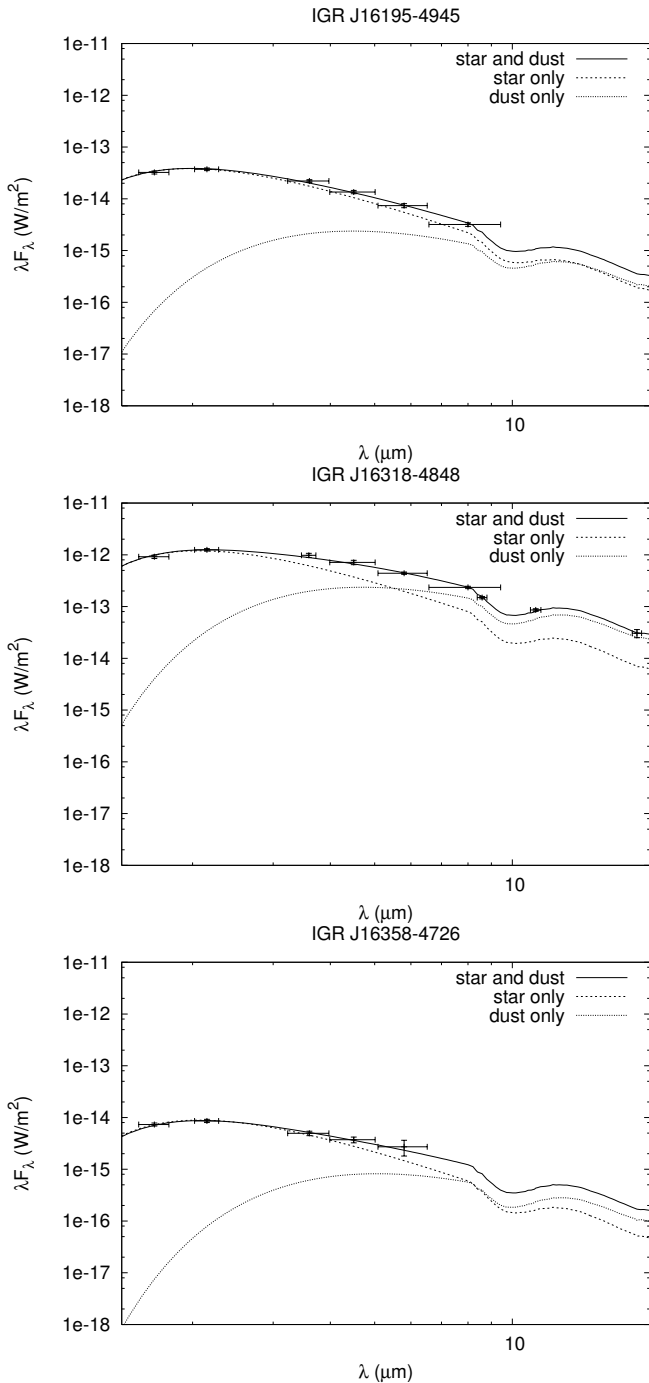


Fig. 4. IR SEDs of IGR J16195-4945, IGR J16318-4848, and IGR J16358-4726 in the NIR and the MIR. We show their SEDs including the contribution of the star and the dust (line), the star only (dashed-line), and the dust only (dotted-line).

Cassinelli & Ignace (1997) propose that the same effect is important from polar to equatorial regions for rapidly rotating B stars. Indeed, the rapid rotation leads to polar brightening that increases the poles temperature to the hot side of the jump. At the same time, the rotation leading to gravity darkening, the equatorial region may be on the cool side of the jump. Consequently, the wind in the equatorial region is denser than the wind in the polar region. Nevertheless, Pelupessy et al.

(2000) show that the rotational velocity of the star should be very close to its critical value to allow the equatorial wind to reach the density needed to create the disk. However, supergiant stars cannot be close to critical rotational velocity because of probable disruption. Additional mechanisms are therefore needed to allow the supergiant star to reach its critical velocity (see e.g. Owocki 2006). In the particular case of an sgB[e] star in an X-ray binary system, the spin-up should occur during the supergiant phase of the companion, which indicates a different evolutionary stage from other HMXBs.

This disk itself cannot explain the strong MIR excess the sgB[e] stars exhibit. Nevertheless, Bjorkman & Cassinelli (1993) have shown the existence of a zone in the disk (about 50-60 stellar radii from the star) in which the temperature is below the temperature of sublimation of the dust (about 1500 K) and the density high enough to allow for its creation.

IGR J16318-4848 is the source in our sample that exhibits the strongest MIR excess, and we believe it is due to the sgB[e] nature of its companion star. Indeed, many other strongly absorbed sources in our sample do not present any MIR excess.

Moreover, it is suggested that IGR J16358-4726, the second source in our sample that exhibits a MIR excess and whose SED needs an additional component to be properly fitted is an sgB[e], because its spectrum has all the characteristic features of supergiant stars plus the [Fe II] feature (CHA08). Our fit is therefore in good agreement with their result, and the only other source of our sample that definitely exhibits a MIR excess is indeed an sgB[e] star.

In the case of IGR J16195-4945, we are more cautious concerning the presence of warm dust that could be responsible for a MIR excess, as we lack data above 8 μm . Indeed, Fig 4. shows that these source could exhibit a MIR excess, but one much lower than the other two. Nevertheless, if this excess were to be confirmed, we believe it would be also due to the sgB[e] nature of the companion.

We would like to point out that, because the dust is most located in an equatorial disk in an sgB[e] star, the simple model we used to fit the SEDs cannot reproduce the complex distribution of the dust around these stars. Nevertheless, it allows the detection of a warm MIR excess because of the presence of dust in the stellar winds. Finally, for all the stars in our sample, we cannot exclude the presence of a cold component - responsible for their intrinsic absorption - which we cannot detect because of the lack of data above 20 μm .

4.2. Spectral type and distance

In our sample, six sources are supergiant stars with a known spectral type - IGR J16318-4848 and IGR J16358-4726 are sgB[e], IGR J16465-4507 is a B0.5I, IGR J17391-3021 is an O8Iab(f), IGR J17544-2619 is an O9Ib, and IGR J19140+0951 is a BII - and three are found to be O/B supergiants whose temperatures derived from our fits allow an assessment of the spectral types using the classification given in Martins et al. (2005) and Crowther et al. (2006) for O and B galactic super-

Table 7. Summary of spectral types (SpT) and distances (D_*) derived from our fits for confirmed supergiant stars in our sample. (*) sources with an accurate spectral type found in the literature (\dagger) confirmed supergiant stars whose temperature derived from our fits was used to assess their accurate spectral type. References to the determination of the spectral type and/or spectral class of these sources are found in Table 1.

Sources	SpT	D_* (kpc)
IGR J16318-4848*	sgB[e]	~ 1.6
IGR J16320-4751 \dagger	O8I	~ 3.5
IGR J16358-4726*	sgB[e]	~ 18.5
IGR J16465-4507*	B0.5I	~ 9.4
IGR J16479-4514 \dagger	O8.5I	~ 4.9
IGR J17252-3616 \dagger	O8.5I	~ 6.1
IGR J17391-3021*	O8I	~ 2.7
IGR J17544-2619*	O9I	~ 3.6
IGR J19140+0951*	B1I	~ 3.1

Table 8. Summary of the distances (D_*) derived from our fits for sources with unconfirmed spectral classes.

Sources	SpT	D_* (kpc)		
		V	III	I
IGR J16195-4945	B1	~ 3.1	~ 5.7	~ 9.8
IGR J16207-5129	O7.5	~ 1.8	~ 2.8	~ 4.1
IGR J16418-4532	O8.5	~ 4.9	~ 8.3	~ 13

giants, respectively, given the uncertainties of observational results (~ 2000 K) and uncertainties on the fits temperatures as given in Table 6. We therefore found that IGR J16320-4751 could be an O8I and IGR J16479-4514 and IGR J17252-3616 could be O8.5I stars.

Concerning the last three sources whose spectral class is unknown, results of the fits listed in Tables 5 and 6 show that they are probably all O/B massive stars, and we also used their derived temperatures to assess their spectral type using the classification given in both papers quoted above. IGR J16195-4945 could be a B1 star, and as already stressed above, it could be an sgB[e] due to its MIR excess, IGR J16207-5129 and IGR J16418-4532 could be O7.5-O8.5 stars. Nevertheless, even if the high intrinsic X-ray absorption of their associated compact objects points towards a supergiant nature since the accretion is likely to be wind-fed, the fits themselves do not allow an assessment of their spectral classes. We then consider they could be either main sequence, giant, or supergiant stars.

Martins & Plez (2006) give a UVJHK synthetic photometry of galactic OI, OIII, and OV stars, with which one can get the expected unabsorbed absolute magnitude in J band M_J for stars having a given spectral classification. Using the absorbed apparent magnitudes m_J of our sources and the J band absorption we derived from our fits, $A_J = 0.289 \times A_V$, it is then

possible to assess the distance of O stars in our sample using the standard relation:

$$D_* = 10^{0.2(m_J - A_J - M_J + 5)} \quad \text{in pc}$$

We did not find any synthetic photometry for B supergiants. Nevertheless, expected radii of galactic BI, BIII, and BV stars are given in Vacca et al. (1996), and we divided these values by the $\frac{R_*}{D_*}$ ratio derived from our fits to get the star distance. The derived distances for the sources whose spectral class is known are listed in Table 7, in Table 8 for the others.

4.3. X-ray properties

Except in the case of IGR J17544-2619, X-ray absorptions are systematically significantly larger than the visible absorptions. This indicates the presence in the system of a two-component absorbing material: one around the companion star, responsible for the visible absorption, and a very dense one around the compact object coming from the stellar winds that accrete onto the compact object and are responsible for the huge X-ray absorption those sources exhibit.

The obscuration of the compact object by the stellar wind is caused by the photoelectric absorption of the X-ray emission by the wind, and this absorption varies along the orbit of the compact object. This orbital dependence has for instance been observed and modelled on 4U 1700-37 (Haberl, White, & Kallman 1989).

Moreover, an effect on the X-ray absorption by the photoionisation of the stellar wind in the vicinity of the compact object by its X-ray emission was predicted by Hatchett & McCray (1977). Indeed, in SGXBs, the compact object moves through the stellar wind of the companion star, and the X-rays are responsible for the enhancement or the depletion of the ionised atoms responsible for the acceleration of the wind (e.g. C IV and N V). This has a direct consequence on the velocity profile of the wind; when the wind enters into an ionised zone, it follows a standard CAK law until it reaches a location in which it is enough ionised for no further radiative driving to take place, and the wind velocity is “frozen” to a constant value from this point. This results in a lower wind velocity close to the compact object and consequently a higher wind density that leads to a higher obscuration of the compact object.

Most of the sources studied in this work are very absorbed in the high-energy domain. Nevertheless, this absorption may not be always that high. In the case of very wide eccentric orbits, the column density of the sources could normally vary along their orbit and suddenly increase when very close to the companion star because of the wind ionisation. In contrast, if these objects were to be always very absorbed, it could mean that their orbit is very close to the companion star and weakly eccentric. If this effect were to be observed, we think it could explain the difference in behaviour between obscured SGXBs (close quasi-circular orbits) and SFXTs (wide eccentric orbits).

Table 9. Sample of parameters we used to fit the SEDs of the isolated supergiants. We give their galactic coordinates, their spectral types, the interstellar extinction in magnitudes A_i and then the parameters themselves: the extinction in the optical A_V , the temperature T_* and the $\frac{R_*}{D_*}$ ratio of the star.

Sources	l	b	SpT	A_i	A_V	$T_*(K)$	$\frac{R_*}{D_*}$
HD 144969	333.18	2.0	B0.5Ia	3.34	3.9	26000	4.01×10^{-10}
HD 148422	329.92	-5.6	B0.5Ib	0.75	0.9	24700	8.76×10^{-11}
HD 149038	339.38	2.51	B1Ia	0.81	1	24000	5.30×10^{-10}
HD 151804	343.62	1.94	O8Iaf	0.83	1.3	32000	4.20×10^{-10}
HD 152234	343.46	1.22	B0.5Ia	1.17	1.5	25100	4.94×10^{-10}
HD 152235	343.31	1.1	B1Ia	3.37	3.9	24500	1.13×10^{-9}
HD 152249	343.35	1.16	O9Ib	1.34	1.7	30100	2.89×10^{-10}
HD 156201	351.51	1.49	B0.5Ia	2.68	2.9	26500	2.90×10^{-10}

4.4. Optical properties

We were able to fit all but three sources with a simple stellar black body model. For these three sources, we explained that the MIR excess was probably caused by the warm dust created within the stellar wind due to the sgB[e] nature of the companions. Therefore, it seems that the optical-to-MIR wavelength emission of these SGXBs corresponds to the emission of absorbed blue supergiants or sgB[e].

Moreover, the results of the fits listed in the Table 5 show that it is *a priori* impossible to differentiate an obscured SGXB and an SFXT from their optical-to-MIR wavelength SEDs, and it then seems that the difference in behaviour between both kinds of SGXBs only depends on the geometry of the system, i.e. its orbital distance or its orbit eccentricity (Chaty & Rahoui 2007).

Nevertheless, to assess a possible effect of the compact object on the companion star, we took a sample of eight isolated O/B supergiants in the direction of the Galactic centre and fitted their optical-to-NIR wavelength SEDs with an absorbed stellar black body. The best-fitting parameters are listed in Table 9 along to their galactic coordinates, their spectral types and the interstellar H I absorption (A_i). The distances of these supergiants are known, which allowed us to calculate A_i out to their position using the tool available on the MAST website (Fruscione et al. 1994).

We see that their visible absorption is of the same order of magnitude as the interstellar H I absorption and well below the level of absorption of our sources. This could mean that some supergiant stars in SGXBs exhibit an excess of absorption due to a local absorbing component. Unfortunately, the total interstellar absorption out to the distance of our sources is unknown, and we cannot compare their visible absorptions derived from our fits to the total interstellar absorption out to their position.

Nevertheless, if this was the case, we think that this excess of absorption could also be caused partly by the photoionisation of the wind in the vicinity of the companion star by the high-energy emission of the compact object, as this would

make their winds slower than in isolated supergiant stars. Since the wind velocity is lower, the medium is denser and suitable for creating a more absorbant material.

Indeed, in the case of persistent sources with very close and quasi-circular orbits, we think that this possible effect could be particularly strong, since the wind around the companion star would be permanently photoionised and would have lower velocities than in isolated supergiants. This could be the general scheme of obscured SGXBs.

On the other hand, in the case of very wide and eccentric orbits, the compact object would be most of the time far from the secondary and its X-ray emission would not photoionise the wind close to the companion star, which would not exhibit any visible absorption excess until the compact object got closer. This could be the general scheme of SFXTs.

At last, in both cases, it would be possible to observe a variation in the P-Cygni profiles of the companion star (i.e. a variation in the wind velocity) with the phase angle of the compact object along its orbit.

As a possible confirmation of this general behaviour, we point out that the visible absorptions derived from our fits for the companion stars of the only sources in our sample that surely exhibit the SFXT behaviour (IGR J16465-4945, IGR J17391-3021, and IGR J17544-2619) are far smaller than the visible absorptions of the others. Moreover, concerning obscured SGXBs, the wind velocity of IGR J16318-4848 was found to be $\sim 410 \text{ km s}^{-1}$ (Filliatre & Chaty 2004), far lower than the expected wind velocity for O/B supergiants ($\sim 1000\text{-}2000 \text{ km s}^{-1}$).

5. Conclusions

In this paper, we presented results of observations performed at ESO/VLT with VISIR, which aimed at studying the MIR emission of twelve *INTEGRAL* obscured HMXBs, whose companions are confirmed or candidate supergiants. Moreover, using the observations performed at ESO/NTT and reported in the companion paper (CHA08), previous optical/NIR observations found in the literature and archival data from USNO, 2MASS, and GLIMPSE, we fitted the broad-band SEDs of these sources using a simple two-component black body model in order to obtain their visible absorptions and temperatures, and to assess the contribution of their enshrouding material in their emission.

We confirmed that all these sources were likely O/B supergiant stars and that, for most of them, the enshrouding material marginally contributed to the emission. Moreover, in the case of IGR J16318-4848, IGR J16358-4726, and perhaps IGR J16195-4945, the MIR excess could be explained by the sgB[e] nature of the companion stars.

By comparing the optical and high-energy characteristics of these sources, we showed that the distinction SFXTs/obscured SGXBs does not seem to exist from optical-to-MIR wavelength. Nevertheless, most of the sources in our sample are significantly absorbed in the optical, and we think that the wind can be denser around some supergiants in SGXBs, which could be due to the photoionisation by the

high-energy emission of the compact object.

Several improvements in our study are needed to allow definitive conclusions. Indeed, the data used to perform the SEDs were not taken simultaneously, which can for instance lead to an incorrect assessment of the MIR excess in the emission. Moreover, the lack of optical magnitudes for several sources could have led to an incorrect fitting of their intrinsic visible absorption A_V . Finally, the absence of an accurate measurement of the total interstellar absorption out to the distance of these sources does not allow us to say whether the presence of the compact object can lead to a stellar wind denser in some supergiants belonging to SGXBs than in isolated supergiants.

We then recommend further optical investigations of these sources to study any possible variation in their P-cygni profile with the phase of the compact object. We also think that the measurement of the distance of these sources is crucial to allow a good assessment of the real interstellar absorption up to their distance, in order to detect any local absorbing component around companion stars. Finally, we recommend X-ray monitoring so as to study the dependence of their column density on orbital phase angle, which could help for understanding the difference between obscured SGXBs and SFXTs.

Acknowledgements. We are pleased to thank Jérôme Rodriguez for his very useful website in which all the *INTEGRAL* sources are referenced (<http://isdc.unige.ch/~rodrigue/html/igrsources.html>).

Based on observations carried out at the European Southern Observatory, Chile (through programmes ID. 075.D-0773 and 077.D-0721). This research has made use of NASA's Astrophysics Data System, of the SIMBAD and VizieR databases operated at the CDS, Strasbourg, France, of products from the US Naval Observatory catalogues, of products from the Two Micron All Sky Survey, which is a joint project of the University of Massachusetts and the Infrared Processing and Analysis Center/California Institute of Technology, funded by the National Aeronautics and Space Administration and the National Science Foundation as well as products from the Galactic Legacy Infrared Mid-Plane Survey Extraordinaire, which is a *Spitzer Space Telescope* Legacy Science Program.

References

- Benjamin, R. A., Churchwell, E., Babler, B. L., et al. 2003, *PASP*, 115, 953
- Bird, A. J., Malizia, A., Bazzano, A., et al. 2007, *ApJS*, 170, 175
- Bjorkman, J. E. & Cassinelli, J. P. 1993, *ApJ*, 409, 429
- Bodaghee, A., Courvoisier, T. J.-L., Rodriguez, J., et al. 2007, *A&A*, 467, 585
- Bohlin, R. C., Savage, B. D., & Drake, J. F. 1978, *ApJ*, 224, 132
- Cardelli, J. A., Clayton, G. C., & Mathis, J. S. 1989, *ApJ*, 345, 245
- Cassinelli, J. P. & Ignace, R. 1997, in *Astronomical Society of the Pacific Conference Series*, Vol. 120, *Luminous Blue Variables: Massive Stars in Transition*, ed. A. Nota & H. Lamers, 166–+
- Castor, J. I., Abbott, D. C., & Klein, R. I. 1975, *ApJ*, 195, 157
- Chaty, S. & Rahoui, F. 2007, *Proceeding of the VIth INTEGRAL Workshop, "The Obscured Universe"*, Space Research Institute, Moscow, Russia, 2006, ESA's Publications Division: Special Publication SP-622
- Chaty, S., Rahoui, F., Foellmi, C., et al. 2008, *ArXiv e-prints*, in press in *A&A*, 802
- Corbet, R. H. D., Hannikainen, D. C., & Remillard, R. 2004, *The Astronomer's Telegram*, 269, 1
- Courvoisier, T. J.-L., Walter, R., Rodriguez, J., Bouchet, L., & Lutovinov, A. A. 2003, *IAU Circ.*, 8063, 3
- Crowther, P. A., Lennon, D. J., & Walborn, N. R. 2006, *A&A*, 446, 279
- Dame, T. M., Hartmann, D., & Thaddeus, P. 2001, *ApJ*, 547, 792
- Dickey, J. M. & Lockman, F. J. 1990, *ARA&A*, 28, 215
- Filliatre, P. & Chaty, S. 2004, *ApJ*, 616, 469
- Fruscione, A., Hawkins, I., Jelinsky, P., & Wiercigroch, A. 1994, *ApJS*, 94, 127
- González-Riestra, R., Oosterbroek, T., Kuulkers, E., Orr, A., & Parmar, A. N. 2004, *A&A*, 420, 589
- Haberl, F., White, N. E., & Kallman, T. R. 1989, *ApJ*, 343, 409
- Hannikainen, D. C., Rawlings, M. G., Muhli, P., et al. 2007, *MNRAS*, 380, 665
- Hannikainen, D. C., Rodriguez, J., & Pottschmidt, K. 2003, *IAU Circ.*, 8088, 4
- Hatchett, S. & McCray, R. 1977, *ApJ*, 211, 552
- Indebetouw, R., Mathis, J. S., Babler, B. L., et al. 2005, *ApJ*, 619, 931
- in't Zand, J. J. M. 2005, *A&A*, 441, L1
- in't Zand, J. J. M., Jonker, P. G., Nelemans, G., Steeghs, D., & O'Brien, K. 2006, *A&A*, 448, 1101
- Kaplan, D. L., Moon, D.-S., & Reach, W. T. 2006, *ApJ*, 649, L107
- Kouveliotou, C., Patel, S., Tennant, A., et al. 2003, *IAU Circ.*, 8109, 2
- Kraus, M. & Miroshnichenko, A. S., eds. 2006, *Astronomical Society of the Pacific Conference Series*, Vol. 355, *Stars with the B[e] Phenomenon*
- Lagage, P. O., Pel, J. W., Authier, M., et al. 2004, *The Messenger*, 117, 12
- Lamers, H. J. G. & Pauldrach, A. W. A. 1991, *A&A*, 244, L5
- Lamers, H. J. G. L. M., Zickgraf, F.-J., de Winter, D., Houziaux, L., & Zorec, J. 1998, *A&A*, 340, 117
- Lebrun, F., Leray, J. P., Lavocat, P., et al. 2003, *A&A*, 411, L141
- Lutovinov, A., Rodrigues, J., Budtz-Jorgensen, C., Grebenev, S., & Winkler, C. 2004, *The Astronomer's Telegram*, 329, 1
- Lutovinov, A., Rodriguez, J., Revnivtsev, M., & Shtykovskiy, P. 2005, *A&A*, 433, L41
- Lutz, D., Feuchtgruber, H., Genzel, R., et al. 1996, *A&A*, 315, L269
- Martins, F. & Plez, B. 2006, *A&A*, 457, 637
- Martins, F., Schaerer, D., & Hillier, D. J. 2005, *A&A*, 436, 1049
- Matt, G. & Guainazzi, M. 2003, *MNRAS*, 341, L13
- Mill, J. D. 1994, in *Presented at the Society of Photo-Optical Instrumentation Engineers (SPIE) Conference*, Vol. 2232,

- Proc. SPIE Vol. 2232, p. 200-216, Signal Processing, Sensor Fusion, and Target Recognition III, Ivan Kadar; Vibeke Libby; Eds., ed. I. Kadar & V. Libby, 200–216
- Molkov, S., Mowlavi, N., Goldwurm, A., et al. 2003, *The Astronomer's Telegram*, 176, 1
- Moneti, A., Stolovy, S., Blommaert, J. A. D. L., Figer, D. F., & Najarro, F. 2001, *A&A*, 366, 106
- Moon, D.-S., Kaplan, D. L., Reach, W. T., et al. 2007, *ApJ*, 671, L53
- Negueruela, I. & Schurch, M. P. E. 2007, *A&A*, 461, 631
- Negueruela, I., Smith, D. M., & Chaty, S. 2005, *The Astronomer's Telegram*, 429, 1
- Negueruela, I., Smith, D. M., Harrison, T. E., & Torrejón, J. M. 2006a, *ApJ*, 638, 982
- Negueruela, I., Smith, D. M., Reig, P., Chaty, S., & Torrejón, J. M. 2006b, in *ESA Special Publication*, Vol. 604, *The X-ray Universe 2005*, ed. A. Wilson, 165–170
- Nespoli, E., Fabregat, J., & Mennickent, R. 2007, *The Astronomer's Telegram*, 983, 1
- Oudmajer, R. D. & Drew, J. E. 1999, *MNRAS*, 305, 166
- Owociki, S. 2006, in *Astronomical Society of the Pacific Conference Series*, Vol. 355, *Stars with the B[e] Phenomenon*, ed. M. Kraus & A. S. Miroshnichenko, 219–+
- Patel, S. K., Kouveliotou, C., Tennant, A., et al. 2004, *ApJ*, 602, L45
- Patel, S. K., Zurita Heras, J., Del Santo, M., et al. 2006, in *Bulletin of the American Astronomical Society*, Vol. 38, *Bulletin of the American Astronomical Society*, 338–+
- Pellizza, L. J., Chaty, S., & Negueruela, I. 2006, *A&A*, 455, 653
- Pelupessy, I., Lamers, H. J. G. L. M., & Vink, J. S. 2000, *A&A*, 359, 695
- Revnitsev, M., Tuerler, M., Del Santo, M., et al. 2003, *IAU Circ.*, 8097, 2
- Rieke, G. H. & Lebofsky, M. J. 1985, *ApJ*, 288, 618
- Rieke, G. H., Rieke, M. J., & Paul, A. E. 1989, *ApJ*, 336, 752
- Rodriguez, J. 2003, *The Astronomer's Telegram*, 194, 1
- Rodriguez, J., Cabanac, C., Hannikainen, D. C., et al. 2005, *A&A*, 432, 235
- Rodriguez, J., Tomsick, J. A., Foschini, L., et al. 2003, *A&A*, 407, L41
- Sguera, V., Barlow, E. J., Bird, A. J., et al. 2005, *A&A*, 444, 221
- Sguera, V., Bazzano, A., Bird, A. J., et al. 2006, *ApJ*, 646, 452
- Shore, S. N. & Sanduleak, N. 1983, *ApJ*, 273, 177
- Shore, S. N., Sanduleak, N., & Allen, D. A. 1987, *A&A*, 176, 59
- Sidoli, L., Vercellone, S., Mereghetti, S., & Tavani, M. 2005, *A&A*, 429, L47
- Smith, D. M., Heindl, W. A., Markwardt, C. B., et al. 2006, *ApJ*, 638, 974
- Sugizaki, M., Mitsuda, K., Kaneda, H., et al. 2001, *ApJS*, 134, 77
- Sunyaev, R., Lutovinov, A., Molkov, S., & Deluit, S. 2003, *The Astronomer's Telegram*, 181, 1
- Swank, J. H. & Markwardt, C. B. 2003, *The Astronomer's Telegram*, 128, 1
- Tomsick, J. A., Chaty, S., Rodriguez, J., et al. 2006, *ApJ*, 647, 1309
- Tomsick, J. A., Lingenfelter, R., Corbel, S., Goldwurm, A., & Kaaret, P. 2004, *The Astronomer's Telegram*, 224, 1
- Tomsick, J. A., Lingenfelter, R., Walter, R., et al. 2003, *IAU Circ.*, 8076, 1
- Tovmassian, G., Tomsick, J. A., & Mennickent, R. 2006, *The Astronomer's Telegram*, 804, 1
- Ubertini, P., Lebrun, F., Di Cocco, G., et al. 2003, *A&A*, 411, L131
- Vacca, W. D., Garmany, C. D., & Shull, J. M. 1996, *ApJ*, 460, 914
- Walter, R., Bodaghee, A., Barlow, E. J., et al. 2004, *The Astronomer's Telegram*, 229, 1
- Walter, R., Rodriguez, J., Foschini, L., et al. 2003, *A&A*, 411, L427
- Walter, R., Zurita Heras, J., Bassani, L., et al. 2006, *A&A*, 453, 133
- Winkler, C., Courvoisier, T. J.-L., Di Cocco, G., et al. 2003, *A&A*, 411, L1
- Zickgraf, F.-J. 1999, in *Lecture Notes in Physics*, Berlin Springer Verlag, Vol. 523, *IAU Colloq. 169: Variable and Non-spherical Stellar Winds in Luminous Hot Stars*, ed. B. Wolf, O. Stahl, & A. W. Fullerton, 40–+
- Zickgraf, F.-J., Wolf, B., Stahl, O., Leitherer, C., & Klare, G. 1985, *A&A*, 143, 421
- Zurita Heras, J. A., de Cesare, G., Walter, R., et al. 2006, *A&A*, 448, 261
- Zurita Heras, J. A. & Walter, R. 2004, *The Astronomer's Telegram*, 336, 1

Note added in proof: After the submission of this paper, Moon et al. (2007) reported MIR spectroscopy of IGR J16318-4848, confirming the presence of two components of warm and cold dust around the supergiant B[e] companion star. Moreover, Hannikainen et al. (2007) reported a more accurate B0.5Ia spectral type of IGR J19140+0951.